

# In search of theoretically predicted magic clusters: Lithium-doped aluminum cluster anions

O. C. Thomas, W.-J. Zheng, T. P. Lippa, S.-J. Xu, S. A. Lyapustina, and K. H. Bowen, Jr.<sup>a)</sup>

*Department of Chemistry, Johns Hopkins University, Baltimore, Maryland 21218*

(Received 9 January 2001; accepted 22 February 2001)

Lithium-doped aluminum cluster anions,  $\text{LiAl}_n^-$  were generated in a laser vaporization source and examined via mass spectrometry and anion photoelectron spectroscopy ( $n=3-15$ ). The mass spectrum of the  $\text{LiAl}_n^-$  series exhibits a local minimum in intensity at  $n=13$ . The electron affinity vs cluster size trend also shows a dip at  $n=13$ . Agreement is quite good between our measured electron affinity values and those calculated by Rao, Khanna, and Jena, suggesting that their predictions about the structure and bonding of  $\text{LiAl}_{13}$  and other clusters in this series are also largely valid. © 2001 American Institute of Physics. [DOI: 10.1063/1.1365110]

## I. INTRODUCTION

Inspired by the discoveries of fullerenes<sup>1</sup> and metallocarbohedrenes<sup>2</sup> in molecular beams, several theorists set out in search of other unusually stable aggregates (magic clusters) that might serve as building blocks for cluster-assembled materials. They reasoned that if such exotic substances could be formed, they might well exhibit unique chemical and physical properties, and that these could lead in turn to novel technological applications.

Among the candidate systems to have been considered by theory,  $\text{MAl}_{13}$  and its analogs ( $M$ =alkali atom) are especially intriguing. Several years ago, calculations by Khanna and Jena<sup>3,4</sup> implied that  $\text{KAl}_{13}$  clusters should form an extended ionic solid in the bulk, analogous to that formed by alkali halide salts. The ionic nature of the  $\text{K}^+\text{Al}_{13}^-$  “molecule” depends substantially on the fact that  $\text{Al}_{13}^-$  is itself a magic cluster, and that it mimics the electronic behavior of an atomic halogen anion. The special stability of  $\text{Al}_{13}^-$  derives from two main factors. It possesses electronic stability because it is a 40 valence electron, closed-shell species, and it has geometrical stability because it is an icosahedron.<sup>5</sup> Also, experiments have shown that  $\text{Al}_{13}^-$  is virtually inert to reaction,<sup>6</sup> and that the electron affinity of  $\text{Al}_{13}$  is close to that of the chlorine atom (both are 3.6 eV).<sup>7</sup> Thus, with its nearly spherical shape and its delocalized valence electron cloud (aluminum is a good free-electron metal),  $\text{Al}_{13}^-$  can be envisioned as a rather stable, albeit larger than usual, pseudohalogen atomic anion with the capability of playing the role of a halogen anion in alkali halide salts. As proposed by Khanna and Jena,  $\text{KAl}_{13}$  is just one example among a number of possible systems in which magic clusters act as new, substitute “atoms,” giving the periodic table a third dimension.<sup>8</sup> Since they first introduced the idea, theoretical work both by these investigators<sup>9,10</sup> and by others<sup>11-14</sup> has been extended beyond  $\text{KAl}_{13}$  to include  $\text{MAl}_{13}$  systems in which  $M$ =Li, Na, Rb, and Cs.

In the present paper, we focus on the lithium/aluminum cluster system. In the bulk, even relatively low concentrations of lithium in aluminum yield alloys which are strong, light, and hard. These alloys are utilized as aerospace structural materials and as electrodes in high energy density batteries. The physical properties of lithium/aluminum alloys stem from the unusual bonding characteristics of lithium/aluminum intermetallic compounds.<sup>15,16</sup> Studies of lithium/aluminum interactions in the finite-size regime of the cluster world may shed additional light on the microscopic basis for the properties of these alloys.

Calculations on lithium/aluminum clusters have proven invaluable in investigating the nature of lithium-doped aluminum clusters,  $\text{LiAl}_n$ , and their anions. Landman and co-workers<sup>17</sup> performed calculations on lithium-rich aluminum clusters, finding  $\text{Li}_5\text{Al}$  to be very stable. They also found  $\text{Li}_{10}\text{Al}_2$  to be composed of two slightly distorted  $\text{Li}_5\text{Al}$  subunits loosely bonded to one another and  $\text{Li}_{20}\text{Al}_4$  likewise to be made up of four  $\text{Li}_5\text{Al}$  subunits. Calculations by Kanhere and co-workers<sup>11</sup> on  $\text{LiAl}_n$  clusters ( $n=1-13$ ) found the lithium atom to sit outside the aluminum cage in each case. They also found that  $\text{Li}_{20}\text{Al}_{13}$  showed special stability.<sup>12</sup> Calculations by Kumar<sup>13</sup> considered several lithium/aluminum clusters, including  $\text{LiAl}_{13}$ , where he too found the lithium atom to lie outside the aluminum cage. Kumar’s work, however, emphasized the properties of  $\text{Li}_8\text{Al}_{10}$ , which he found to be a layered compound cluster with ionic bonding between its aluminum and lithium layers. Especially extensive calculations on lithium-doped aluminum clusters were conducted by Rao, Khanna, and Jena.<sup>9,10,18</sup> While they studied a variety of sizes and compositions, their focus was on structure and bonding in  $\text{LiAl}_{13}$  and its immediate-sized neighbors. These investigators found  $\text{LiAl}_{13}$  to exhibit the same structure as the other  $\text{MAl}_{13}$  clusters, i.e., with the lithium atom residing outside of an aluminum cage. Its bonding, on the other hand, deviated somewhat from the picture painted above for  $\text{KAl}_{13}$ . While classified as

<sup>a)</sup>Author to whom correspondence should be addressed. Electronic mail: kitbowen@jhunix.hcf.jhu.edu

ionic, the bonding in  $\text{LiAl}_{13}$  was found to be much less so than the other members of the  $\text{MAl}_{13}$  family. In order to provide specific checkpoints for experiment, Rao and co-workers also computed binding energies, ionization potentials, and electron affinities for these species. In the present paper, we have contributed toward the characterization of  $\text{LiAl}_n$  clusters and their anions by recording the mass spectra of the  $\text{Li}_m\text{Al}_n^-$  homologous series and the negative ion photoelectron spectra of  $\text{LiAl}_n^-$ ,  $n = 3-15$ , the latter providing electron affinities.

## II. EXPERIMENT

Negative ion photoelectron spectroscopy is conducted by crossing a mass-selected beam of anions with a fixed-frequency photon beam and energy analyzing the resultant photodetached electrons. This technique is governed by the following energy-conserving relationship:

$$h\nu = \text{EKE} + \text{EBE}, \quad (1)$$

where  $h\nu$  is the photon energy, EKE is the measured electron kinetic energy, and EBE is the electron binding energy.

In the present experiments, both mass spectra and the anion photoelectron (photodetachment) spectra were collected on an apparatus consisting of a laser vaporization source, a linear time-of-flight mass spectrometer for mass analysis and mass selection, and a magnetic bottle photoelectron spectrometer for electron energy analysis. The ion source consists of a Smalley-style laser vaporization source which utilizes a pulsed gas valve, a rotating and translating sample rod made of an aluminum/lithium alloy,<sup>19</sup> and second harmonic light pulses from a Nd:YAG laser. The cluster anions of interest were generated under two sets of source conditions, one utilizing essentially no helium in its expansion and the other using a laser vaporization block of different geometry and  $\sim 4$  atm of helium gas behind its pulsed valve. We found the "no helium" condition to give higher intensities for the smaller  $\text{LiAl}_n^-$  cluster anions, while the larger sizes that we studied required the "with helium" condition in order to produce significant intensities. In both cases, the source was aimed perpendicularly into the Wiley-McLaren extraction region of our time-of-flight mass spectrometer. Deflectors and an Einzel lens were positioned immediately downstream of the extraction plates. Just before the anions passed through the ion-photon interaction region, they encountered a mass gate followed by a momentum decelerator. Immediately after the ion-photon interaction region, a Channeltron electron multiplier monitored the arrival of the ions. At the ion-photon interaction region, electrons were photodetached from the anion of interest with the third harmonic of a second Nd:YAG laser. Most of these electrons were then energy analyzed by a magnetic bottle photoelectron spectrometer and detected with a multichannel plate. A LeCroy digital oscilloscope collected the data, which were manipulated with a laboratory computer. The usual resolution of our magnetic bottle electron spectrometer during these experiments was  $\sim 50$  meV at an electron kinetic energy of  $\sim 1$  eV.

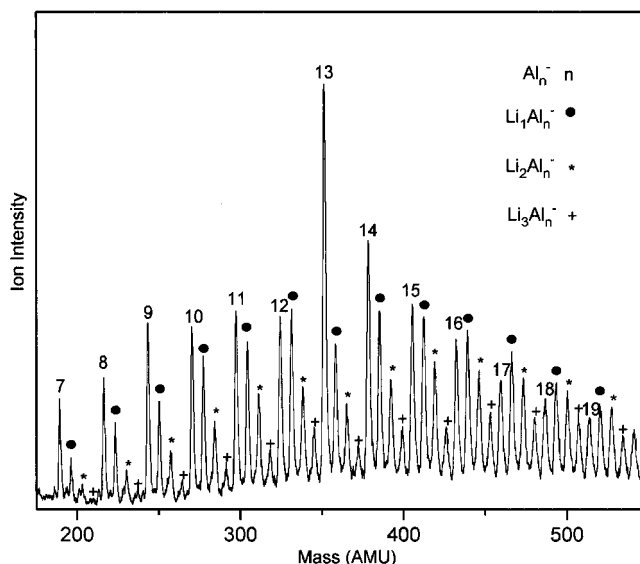


FIG. 1. A typical negative ion mass spectrum resulting from the use of a lithium/aluminum alloy target rod in our laser vaporization source.

## III. RESULTS

### A. Mass spectra

Figure 1 shows a typical mass spectrum resulting from this work when helium was used in the source. Four cluster anion homologous series are evident,  $\text{Al}_n^-$ ,  $\text{LiAl}_n^-$ ,  $\text{Li}_2\text{Al}_n^-$ , and  $\text{Li}_3\text{Al}_n^-$ . The abundance patterns shown here were persistent from day to day. The  $\text{Al}_n^-$  series is dominated by an intense peak at  $\text{Al}_{13}^-$ . The defining feature of the  $\text{LiAl}_n^-$  series is the dip in intensity observed at  $\text{LiAl}_{13}^-$ . Likewise, in both the  $\text{Li}_2\text{Al}_n^-$  and the  $\text{Li}_3\text{Al}_n^-$  series, dips in intensity are also seen at  $n=13$ . These observations can be understood in terms of shell model magic numbers.  $\text{Al}_{13}^-$  is a 40 valence electron, closed-shell species, and is itself expected to be especially stable and abundant.  $\text{LiAl}_{13}^-$  is a 41 valence electron species, and as such it has one electron more than the number needed to form a closed electronic shell. Such a species, with a valence electron number just beyond a closed-shell magic number, would be expected to show a local intensity minimum (a dip) in its mass spectrum. The species,  $\text{Li}_2\text{Al}_{13}^-$  and  $\text{Li}_3\text{Al}_{13}^-$ , possess 42 and 43 valence electrons, respectively. Since this gives them, respectively, 2 and 3 more electrons than are needed to form a closed shell at 40, it is not surprising that they also display intensity dips. When the next smaller member of each series is considered, however, one notices that while  $\text{Li}_2\text{Al}_{12}^-$ , with its 39 valence electrons, is 1 electron short of the closed shell at 40 electrons,  $\text{Li}_3\text{Al}_{12}^-$ , with its 40 valence electrons, is itself a closed shell. While  $\text{Li}_3\text{Al}_{12}^-$  does indeed show a local intensity maximum, interestingly, it is not especially prominent.<sup>20</sup>

### B. Photoelectron spectra

The photoelectron spectra of  $\text{LiAl}_n^-$ ,  $n = 3-15$  are presented in Fig. 2. These spectra were recorded with 3.49 eV photons and calibrated against the well-known transitions of the copper atomic anion. Examination of the spectra shows a general trend in which their onsets shift to successively

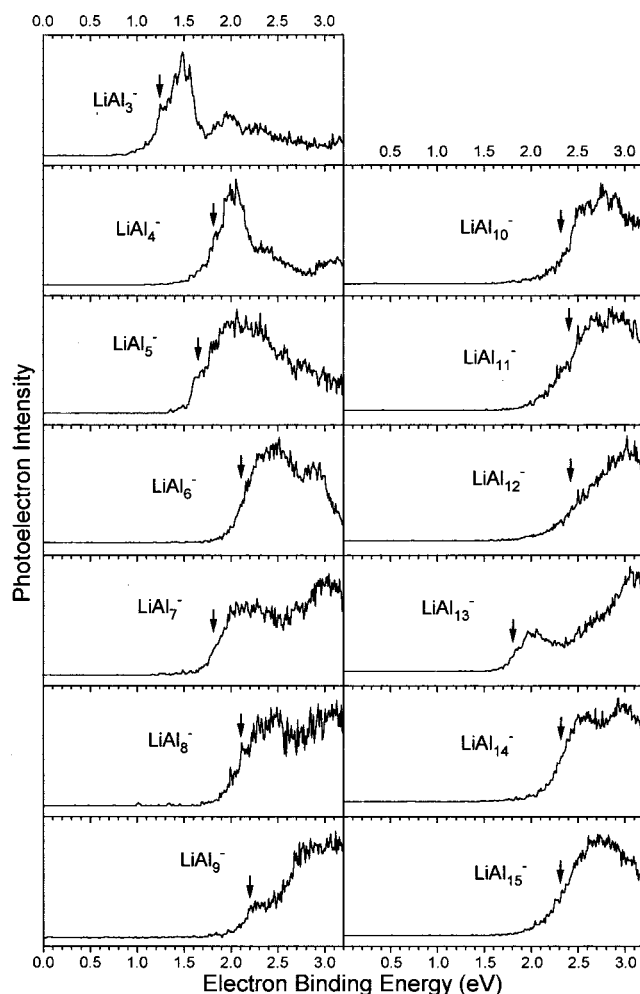


FIG. 2. The photoelectron spectra of  $\text{LiAl}_n^-$ ,  $n=3-15$ , recorded with 3.49 eV photons. The arrows above the spectra indicate the assigned locations of their origins and thus the adiabatic electron affinities of their corresponding neutral  $\text{LiAl}_n$  clusters.

higher electron binding energies (EBEs) with increasing size but with some of them slipping back momentarily to lower EBEs. From  $n=3$  to  $n=4$ , the onset shifts to higher EBE. At  $n=5$ , the onset shifts back slightly to lower EBE before resuming its shift to higher EBE at  $n=6$ . At  $n=7$ , the onset shifts back to lower EBE again, resuming its march to higher EBEs at  $n=8$  and continuing relatively smoothly through  $n=12$ . Then, at  $n=13$ , the spectrum dips back to lower EBE still again, in its case dramatically (by  $\sim 0.6$  eV). After  $n=13$ , the EBEs of the onsets of  $n=14$  and  $n=15$  increase again. In order to generate suitable intensities, the  $\text{LiAl}_n^-$  cluster anions photodetached in these spectra over the size range  $n=3-8$  were generated under source conditions which did not employ helium gas in the expansion, while those photodetached in these spectra over the size range  $n=9-15$  were produced under source conditions which utilized substantial helium in the source expansion. After accounting for the likely effect of hot bands, nominal adiabatic electron affinities, E.A.<sub>a</sub>, for  $\text{LiAl}_n$  clusters were assigned along the steeply rising portion of the low EBE side of each spectrum. These values are presented in Table I and are plotted versus size in

TABLE I. Electron affinities (E.A.) of  $\text{LiAl}_n$  vs cluster size ( $n$ ).

$n$	E.A. (this work) <sup>a</sup>	E.A. (theory) <sup>b</sup>
3	$1.25 \pm 0.10$	1.32
4	$1.80 \pm 0.10$	1.91
5	$1.65 \pm 0.15$	1.76
6	$2.10 \pm 0.15$	2.46
7	$1.80 \pm 0.15$	1.92
8	$2.10 \pm 0.15$	2.21
9	$2.20 \pm 0.20$	...
10	$2.30 \pm 0.15$	...
11	$2.40 \pm 0.20$	...
12	$2.40 \pm 0.20$	2.63
13	$1.80 \pm 0.10$	1.85
14	$2.30 \pm 0.15$	2.37
15	$2.30 \pm 0.15$	...

<sup>a</sup>Electron affinities are given in eV, both for this work and for theory.

<sup>b</sup>References 18, 21.

Fig. 3, where slight dips in the E.A.<sub>a</sub> vs  $n$  trend are seen at  $n=5$  and  $n=7$ , and a more substantial one is evident at  $n=13$ .

#### IV. DISCUSSION

We wish to address two relatively separate aspects of the lithium/aluminum cluster story, one dealing with the nature of  $\text{LiAl}_{13}$  and its relationship to its neighboring size  $\text{LiAl}_n$  clusters and the other involving the properties of the smaller  $\text{LiAl}_n$  clusters. In both, we rely on theoretical guidance provided by the calculations of Rao, Khanna, and Jena.<sup>9,10,18</sup> Below, we compare their predictions with our data. When our experimental results agree with their theoretical results, we interpret this as indicating that their inferences about the structure and bonding of these systems are also probably on the right track.

##### A. $\text{LiAl}_{13}$ and its immediate neighbors

Rao and co-workers characterized the structure of neutral  $\text{LiAl}_{13}$  as a 13 atom aluminum cage with a lithium atom

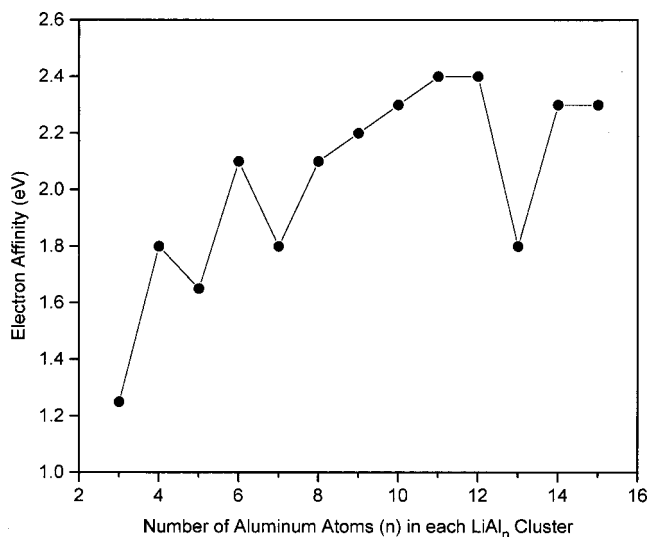


FIG. 3. A plot of the measured electron affinities of  $\text{LiAl}_n$  vs cluster size,  $n$ .

exterior to it. They found two nearly isoenergetic structures for  $\text{LiAl}_{13}$ 's aluminum cage, one decahedral and the other icosahedral, with the latter being slightly lower in energy. These investigators further found the binding energy of Li to  $\text{Al}_{13}$  to be the highest in the  $\text{MAl}_{13}$  series, while the degree of ionicity in the Li– $\text{Al}_{13}$  bond was the lowest in the same series. Their Mulliken charge analysis found very little charge transfer from Li to  $\text{Al}_{13}$ . The charge density contours, on the other hand, did not indicate a covalent bond. As a maverick among the alkali atoms, lithium often shows unusual behavior. In terms of experimentally accessible properties, Rao *et al.* noted that  $\text{LiAl}_{13}$ , as a closed-shell species, should exhibit a higher ionization potential and a lower electron affinity than its immediate-size neighbors, and they calculated values for both as a function of cluster size.

The dip in the intensity of the  $\text{LiAl}_n^-$  mass spectrum at  $n=13$  and the dip in  $\text{LiAl}_n^-$ 's  $E.A._a$  vs  $n$  trend at  $n=13$  are both consistent with neutral  $\text{LiAl}_{13}$  being a closed-shell species with enhanced stability. The main quantitative points of comparison between our data and theoretical results of Rao and co-workers comes through the photoelectron spectra of  $\text{LiAl}_{13}^-$  and its immediate neighbors. The key parameters for comparison are adiabatic electron affinities. Recently, Khanna and co-workers have also provided us with the not-yet-published results of their "all electron" calculations.<sup>21</sup> For  $\text{LiAl}_{13}$ , these calculations gave adiabatic electron affinities ( $E.A._a$ ) of 1.85 and 1.88 eV for those isomers with icosahedral and decahedral aluminum cage geometries, respectively. For  $\text{LiAl}_{13}^-$ , these calculations gave vertical detachment energies (VDE) of 2.05 and 2.15 eV for the icosahedral and decahedral cage geometries, respectively. From the lowest EBE peak (band) in the photoelectron spectrum of  $\text{LiAl}_{13}^-$ , we determined the VDE to be 2.05 eV and the  $E.A._a$  of  $\text{LiAl}_{13}$  to be 1.80 eV, both in excellent agreement with the "all electron" predictions of Khanna, Rao, and Jena. The differences in  $E.A._a$  and VDE values for the two cage geometries are too close for us to use our measurements to distinguish between these isomers. Considering  $\text{LiAl}_{12}^-$  and  $\text{LiAl}_{14}^-$ , the immediate neighbors on either side of  $\text{LiAl}_{13}^-$ , their "all electron" calculations found  $E.A._a$  values for  $\text{LiAl}_{12}$  and  $\text{LiAl}_{14}$  to be 2.63 and 2.37 eV, respectively. (They did not compute VDE values for these.) From the photoelectron spectra of  $\text{LiAl}_{12}^-$  and  $\text{LiAl}_{14}^-$ , we determined the  $E.A._a$  of  $\text{LiAl}_{12}$  to be  $\sim 2.4$  eV and the  $E.A._a$  of  $\text{LiAl}_{14}$  to be 2.3 eV. Because of the shape of the lowest EBE band of the  $\text{LiAl}_{13}^-$  spectrum and the availability of a theoretically predicted VDE value for  $\text{LiAl}_{13}^-$ , we were able to give a more precise value for the  $E.A._a$  of  $\text{LiAl}_{13}$  than for  $\text{LiAl}_{12}$  and  $\text{LiAl}_{14}$  (see Table I). Overall, the agreement between theory and experiment is very good. Qualitatively, the electron affinity of  $\text{LiAl}_{13}$  is lower than its immediate-size neighbors at  $n=12$  and 14, and quantitatively, the numerical match between theory and experiment is quite close.

The remainder of the photoelectron spectrum of  $\text{LiAl}_{13}^-$  also deserves attention. In addition to a clearly defined band centered at an EBE of 2.05 eV, we also observe a band centered at 3.1 eV, and possibly another band (partially obscured) centered at  $\sim 2.6$  eV. All of these bands are interpreted as reflecting the vibronic structure of neutral  $\text{LiAl}_{13}$

measured (vertically) at the geometry of the anion,  $\text{LiAl}_{13}^-$ . Khanna and co-workers have calculated the transition energies not only from the ground state of  $\text{LiAl}_{13}^-$  (a doublet) to the ground state of neutral  $\text{LiAl}_{13}$  (a singlet), but also from the ground state of  $\text{LiAl}_{13}^-$  to the first excited triplet state of neutral  $\text{LiAl}_{13}$ . As mentioned earlier, the former transition energy (the VDE) was found to be 2.05 eV for the icosahedral isomer and 2.15 eV for the decahedral form. The transition energy for the latter transition, however, was found to be 3.3 eV for both isomers. This matches the peak that we see at 3.1 eV reasonably well. Given that calculations by Rao *et al.* have found the structures of neutral  $\text{LiAl}_n$  clusters to be rather similar to those of their corresponding anions, this implies that the ground-state singlet to excited state triplet transition in neutral  $\text{LiAl}_{13}$  is  $\sim 1$  eV. While there is presently no theoretical guidance available about the third weak band at 2.6 eV, it may be a transition to an excited singlet state of neutral  $\text{LiAl}_{13}$ .

Experimental work on related systems also tends to be consistent with the  $\text{MAl}_{13}$  concept and to support the credibility of theoretical computations which have explored it. Nakajima, Kaya, and co-workers<sup>22–24</sup> conducted mass spectral studies on  $\text{NaAl}_n^-$  and  $\text{NaIn}_n^-$ , in both cases finding dips in their ion intensities at  $n=13$ . In addition, they performed ionization potential (I.P.) measurements on neutral  $\text{NaAl}_n$ ,  $\text{CsAl}_n$ , and  $\text{NaIn}_n$  clusters, finding peaks in their I.P. vs  $n$  trends in each case at  $n=13$ . In the case of  $\text{NaAl}_{13}$ , theory by Rao *et al.* predicted its I.P. to be 6.3–6.5 eV, while Nakajima's experimental result gave a lower limit of 6.4 eV. While no theoretical prediction was available for the I.P. of  $\text{CsAl}_{13}$ , its measured I.P. was 6.42 eV, suggesting that the I.P. of  $\text{NaAl}_{13}$  was probably not too much higher than 6.4 eV and implying substantial agreement between theory and Nakajima's experiment. Gantefoer, Seifert, and co-workers<sup>25</sup> conducted anion photoelectron spectroscopy on  $\text{HAL}_{13}^-$ , determining the adiabatic electron affinity of  $\text{HAL}_{13}$  to be 2.0 eV and the HOMO–LUMO gap to be 1.4 eV. Seifert's calculations found the adiabatic electron affinity and the HOMO–LUMO gap to be 1.7 and 1.8 eV, respectively, and also characterized the H– $\text{Al}_{13}$  bond as being covalent. In our own group, we have performed mass spectral and anion photoelectron studies on,  $\text{NaAl}_n^-$ ,  $\text{KAl}_n^-$ ,  $\text{RbAl}_n^-$ ,  $\text{CsAl}_n^-$ , and  $\text{CuAl}_n^-$ . In the case of  $\text{KAl}_n^-$ , we saw a dip in the anion intensity at  $n=13$ , and we measured the adiabatic electron affinity of  $\text{KAl}_{13}$  to be  $\sim 1.4$ – $1.6$  eV.<sup>26</sup> "All electron" calculations by Rao, Khanna, and Jena characterized the K– $\text{Al}_{13}$  bond as highly ionic and found the adiabatic electron affinity of  $\text{KAl}_{13}$  to be 1.54 eV for the icosahedral cage isomer and 1.58 eV for the decahedral cage isomer, in good agreement with our measurements. Despite copper being alkali-like in some ways, our work<sup>27</sup> with  $\text{CuAl}_{13}^-$  found very different behavior than that seen in alkali- and hydrogen- $\text{Al}_{13}$  systems. Instead of a dip in its anion intensity at  $n=13$ , the mass spectrum of  $\text{CuAl}_n^-$  showed a prominent peak at  $n=13$ . Calculations by Khanna and co-workers predicted that the copper atom in this case would sit at the center of the aluminum cage, and this was consistent with our shell model level reordering interpretation of the unexpected magic number at  $n=13$ . In addition, their predicted  $E.A._a$  of 2.16 eV

agreed well with our measured  $E.A._a$  of 2.14 eV. Thus, even when systems which resemble  $MAI_{13}$  deviate from their expected behavior, theory has been successful in predicting and elucidating the deviation.

## B. Smaller $LiAl_n$ clusters

Rao and Jena also calculated the adiabatic electron affinities for small  $LiAl_n$  clusters,  $n = 1-8$ . Our measurements of  $LiAl_n$  electron affinities overlap with these through the size range,  $n = 3-8$ . For  $n = 3-8$ , they found adiabatic electron affinities of 1.32, 1.91, 1.76, 2.46, 1.92, and 2.21 eV, respectively. Over the same size range, we found  $E.A._a$  values of 1.25, 1.8, 1.65, 2.1, 1.8, and 2.1 eV, respectively. The agreement is relatively good, both numerically and in terms of qualitative trends.

Based on calculations of their dissociation energies, Kanhere and co-workers<sup>11</sup> predicted that neutral  $LiAl_3$  and  $LiAl_6$  should show higher stabilities than other small  $LiAl_n$  clusters. Rao and Jena<sup>18</sup> also considered the stabilities of small  $LiAl_n$  clusters but from a different perspective. Wang and co-workers<sup>7</sup> had shown aluminum to be monovalent in aluminum clusters smaller than  $Al_9$ . By using lithium atoms as probes, Rao and Jena addressed the issue of whether small aluminum clusters show electronic shell model properties. This was done by calculating several properties of  $LiAl_n$  as a function of size and then looking for shell model characteristics. Based on the behavior of most properties examined, they concluded that small aluminum clusters do not behave like free-electron systems. Their  $E.A._a$  calculations, on the other hand, found the  $E.A._a$  of  $LiAl_7$  to be smaller than those of its neighboring clusters, consistent with  $LiAl_7$  being an electronic closed-shell species. In our photoelectron experiments, we also observed the predicted dip in the  $E.A._a$  vs  $n$  trend for  $LiAl_n$  at  $n = 7$ , but we saw no dip in ion intensity at  $n = 7$  in our  $LiAl_n^-$  mass spectra. Rao and Jena doubted the shell closure implication for small  $LiAl_n$  clusters, however, suspecting that the shell model is not valid for such small systems and citing the fact that the electron affinity was the only calculated property they studied that suggested shell model structure. They also noted a similar dip in the  $E.A._a$  vs  $n$  trend for  $LiAl_5$ , a cluster which is not a candidate for shell closure. We saw the same slight dip at  $n = 5$  in our measured  $E.A._a$  vs  $n$  trend and also a dip in local ion intensity at  $n = 5$  in our mass spectra.

Additional species in our mass spectra of  $Li_mAl_n^-$  cluster anions also speak to this issue, although indecisively. Cluster anions which are themselves closed-shell species are expected to show local maxima in ion intensity, whereas cluster anions with one electron more than their closed shell neutral counterparts are expected to show local minima.  $LiAl_6^-$  has 8 valence electrons if one assumes a valency of 1 for aluminum, and it has 20 electrons if one assumes a valency of 3. Since 8 and 20 are both shell closings in the spherical shell model,  $LiAl_6^-$  has the potential of being a closed-shell species. The intensity of  $LiAl_6^-$ , however, is not a local maximum in our low mass range, mass spectra. Next, consider  $Li_2Al_5^-$ . It could qualify as a closed-shell species with either 8 or 18 valence electrons, depending on which

aluminum valency is assumed. The number, 18, is also a spherical shell model shell closing. The same can be said of neutral  $Li_2Al_6$  with either 8 or 20 valence electrons. If  $Li_2Al_5^-$  is a closed shell, it should give a peak in the low mass range, mass spectrum. If neutral  $Li_2Al_6$  is a closed shell,  $Li_2Al_6^-$  should show a dip in the mass spectrum. Interestingly, the ion intensity of  $Li_2Al_5^-$  goes up relative to that of smaller  $Li_2Al_n^-$  species just before it in the mass spectrum and then drops at  $Li_2Al_6^-$  before rising again at  $Li_2Al_7^-$ . Also, let us consider  $Li_3Al_4^-$ . It could be a closed shell with its 8 valence electrons, but no enhanced peak is seen for  $Li_3Al_4^-$  in the mass spectrum. Last, consider neutral  $Li_3Al_5$ . It could be a closed-shell species with either 8 or 18 valence electrons. If so, its anion,  $Li_3Al_5^-$  should exhibit a dip in the mass spectrum, but none is seen. We plan to perform anion photoelectron experiments on multiple lithium, lithium/aluminum cluster anions,  $Li_mAl_n^-$ , especially those with  $n > 10$ .

## V. CONCLUSION

The good agreement between measured and computed electron affinities for  $LiAl_n$  clusters (over the compared size range of  $n = 3-8, 12-14$ ) suggests that theoretical predictions made about the structures and bonding of these clusters are also probably valid. For  $n = 13$ , the accord between theory and our measurements extends beyond its electron affinity to include the low-lying electronic structure of neutral  $LiAl_{13}$  and the vertical detachment energy of  $LiAl_{13}^-$ . Based on this, we conclude that  $LiAl_{13}$  can be viewed as a pseudodiatom "molecule" composed of Li atomic and  $Al_{13}$  cluster moieties, and that its bonding is ionic, albeit only very slightly. Also, given that theory finds the Li- $Al_{13}$  bond to be the strongest in the  $MAI_{13}$  series,  $LiAl_{13}$  may be a candidate as a building block for cluster assembled materials.

## ACKNOWLEDGMENTS

We thank Kevin McHugh for pointing out the availability of lithium/aluminum alloys and KB Alloys for donating an ingot to us. We benefited greatly from discussions with B. K. Rao, S. N. Khanna, and P. Jena about the results of their calculations (both published and unpublished) on  $LiAl_n$  clusters and their anions. This work was supported by the Division of Materials Science, Office of Basic Energy Sciences, U.S. Department of Energy under Grant No. DE-FG0295ER45538. Acknowledgment is also made to The Donors of the Petroleum Research Fund, administered by the American Chemical Society, for partial support of this research (Grant No. 28452-AC6).

<sup>1</sup>H. W. Kroto, J. R. Heath, S. C. O'Brian, R. F. Curl, and R. E. Smalley, *Nature* (London) **318**, 162 (1985).

<sup>2</sup>B. C. Guo, K. P. Kerns, and A. W. Castleman, Jr., *Science* **255**, 1411 (1992).

<sup>3</sup>S. N. Khanna and P. Jena, *Chem. Phys. Lett.* **219**, 479 (1994).

<sup>4</sup>S. N. Khanna and P. Jena, *Phys. Rev. B* **51**, 13705 (1995).

<sup>5</sup>A. Rubio, L. C. Balbas, and J. A. Alonso, *Physica B* **168**, 32 (1991).

<sup>6</sup>R. E. Leuchtner, A. C. Harms, and A. W. Castleman, Jr., *J. Chem. Phys.* **91**, 2753 (1989).

<sup>7</sup>X. Li, H. Wu, X.-B. Wang, and L.-S. Wang, *Phys. Rev. Lett.* **81**, 1909 (1998).

- <sup>8</sup>S. N. Khanna and P. Jena, *Phys. Rev. Lett.* **69**, 1664 (1992).
- <sup>9</sup>B. K. Rao, S. N. Khanna, and P. Jena, *Phys. Rev. B* **62**, 4666 (2000).
- <sup>10</sup>B. K. Rao, S. N. Khanna, and P. Jena, in *Cluster and Nanostructure Interfaces*, edited by P. Jena, S. N. Khanna, and B. K. Rao (World Scientific, Singapore, 2000), p. 317.
- <sup>11</sup>C. Majumder, G. P. Das, S. K. Kulshrestha, V. Shah, and D. G. Kanhere, *Chem. Phys. Lett.* **261**, 515 (1996).
- <sup>12</sup>A. M. Vichare and D. G. Kanhere, *Eur. Phys. J. D* **4**, 89 (1998).
- <sup>13</sup>V. Kumar, *Phys. Rev. B* **60**, 2916 (1999).
- <sup>14</sup>V. Kumar, *Phys. Rev. B* **57**, 8827 (1998).
- <sup>15</sup>X.-Q. Guo, R. Podlucky, and A. J. Freeman, *Phys. Rev. B* **40**, 2793 (1989).
- <sup>16</sup>X.-Q. Guo, R. Podlucky, and A. J. Freeman, *Phys. Rev. B* **42**, 10912 (1990).
- <sup>17</sup>H.-P. Cheng, R. N. Barnett, and U. Landman, *Phys. Rev. B* **48**, 1820 (1993).
- <sup>18</sup>B. K. Rao and P. Jena, *J. Chem. Phys.* **113**, 1508 (2000).
- <sup>19</sup>The alloy we used was composed of ~5% lithium in aluminum and was obtained from KB Alloys, Inc.
- <sup>20</sup>The ion intensity of  $\text{Li}_3\text{Al}_{18}^-$  may exhibit a weak “shelf” in the mass spectrum. If so, this is consistent with the spherical shell model, since  $\text{Li}_3\text{Al}_{18}^-$  has 58 valence electrons, and 58 is a shell closing number.
- <sup>21</sup>S. N. Khanna, B. K. Rao, and P. Jena (private communication).
- <sup>22</sup>A. Nakajima, K. Hoshino, T. Naganuma, Y. Sone, and K. Kaya, *J. Chem. Phys.* **95**, 7061 (1991).
- <sup>23</sup>A. Nakajima, K. Hoshino, T. Sugioka, T. Naganuma, T. Taguwa, Y. Yamada, K. Watanabe, and K. Kaya, *J. Phys. Chem.* **97**, 86 (1993).
- <sup>24</sup>K. Hoshino, K. Watanabe, Y. Konishi, T. Taguwa, A. Nakajima, and K. Kaya, *Chem. Phys. Lett.* **231**, 499 (1994).
- <sup>25</sup>S. Burkart, N. Blessing, B. Klipp, J. Mueller, G. Gantfoer, and G. Seifert, *Chem. Phys. Lett.* **301**, 546 (1999).
- <sup>26</sup>O. C. Thomas, W. Zheng, and K. H. Bowen (unpublished).
- <sup>27</sup>O. C. Thomas, W. Zheng, and K. H. Bowen, *J. Chem Phys.* **114**, 5514 (2001).